

A Bayesian approach to differential prevalence analysis with applications in microbiome studies

Juho Pelto^{1,2}, Kari Auranen^{2,3}, Janne V. Kujala², and Leo Lahti¹

¹*Department of Computing, University of Turku, Finland*

²*Department of Mathematics and Statistics, University of Turku, Finland*

³*Department of Clinical Medicine, University of Turku, Finland*

Abstract

Recent evidence suggests that analyzing the presence/absence of taxonomic features can offer a compelling alternative to differential abundance analysis in microbiome studies. However, standard approaches face challenges with boundary cases and multiple testing. To address these challenges, we developed DiPPER (Differential Prevalence via Probabilistic Estimation in R), a method based on Bayesian hierarchical modeling. We benchmarked our method against existing differential prevalence and abundance methods using data from 67 publicly available human gut microbiome studies. We observed considerable variation in performance across methods, with DiPPER outperforming alternatives by combining high sensitivity with effective error control. DiPPER also demonstrated superior replication of findings across independent studies. Furthermore, DiPPER provides differential prevalence estimates and uncertainty intervals that are inherently adjusted for multiple testing.

Keywords: presence/absence, microbiome, Bayesian statistics, multiple testing, differential abundance

*Corresponding author: jepelt@utu.fi

Introduction

Recent research suggests that using only presence/absence information, rather than complete abundance profiles of taxonomic features (e.g., species or genera) may be sufficient or even advantageous when analyzing associations between microbiomes and external variables such as health outcomes. For example, benchmarking studies have shown that machine learning classifiers maintain their performance when using only the observed presence/absence of taxonomic features when classifying subjects as healthy or non-healthy [1, 2].

In particular, differential prevalence analysis (DPA), which in its simplest form compares feature prevalences between two groups (e.g., healthy vs. non-healthy subjects), represents a compelling alternative to traditional differential abundance analysis (DAA). Empirical evaluations have indicated that many differential abundance signals are driven primarily by prevalence differences [3, 4] and that DPA performs competitively against many DAA methods in terms of sensitivity and reproducibility [5]. Moreover, DPA offers distinct advantages, as its results are more straightforward to interpret while being inherently more robust to compositional effects and feature-specific biases [6, 7, 8].

While DPA can be performed using standard frequentist logistic regression, this approach has certain drawbacks. The first shortcoming stems from its reliance on null hypothesis testing to detect differentially prevalent features among dozens to thousands of candidates. Due to the large number of simultaneous tests, the resulting p-values require artificial post-hoc adjustment to avoid excessive false discoveries. Although multiplicity corrections generally perform well in controlling the false positive rate, they may do so at the cost of an increased number of false negatives. Moreover, such corrections often do not extend straightforwardly to point estimates or confidence intervals.

Another drawback concerns the calculation of p-values and confidence intervals. Their exact computation is infeasible in practice, necessitating reliance on approximations such as the Wald test (default in many statistical software), likelihood ratio test, or penalized likelihood methods [9]. Although these approximations often work well, they may lose accuracy in boundary cases (e.g., when a feature has either 0% or 100% prevalence in one group, see Figure 1), as is typical in microbiome datasets. In particular, the commonly used Wald test fails to yield any p-value in such situations.

An alternative approach to DPA is to employ a Bayesian hierarchical modeling framework. In contrast to frequentist methods, the guiding principle in this approach is not the avoidance of false positives but the accurate estimation of the differential prevalence of each feature by using other features as an additional source of information. This yields point estimates and uncertainty intervals that are naturally adjusted for multiple testing [10, 11], enabling their direct use to identify differentially prevalent features. Moreover, as the point estimates and intervals are regularized, they remain finite even in boundary cases.

Here, we introduce DiPPER (Differential Prevalence via Probabilistic Estimation in R), a DPA method based on Bayesian hierarchical modeling. The method assumes that the differential prevalence of each feature in the data arises from a common prior distribution whose variance and skewness are informed by all features collectively. Notably, we choose an asymmetric Laplace distribution peaked at zero as the prior. This choice is motivated by the natural assumption that true differential prevalence effects are negligible for most taxonomic features, and by our observation that within a given microbiome study, most non-zero prevalence differences tend to share the same direction (see Supplementary Figure 6). Following the introduction of our model, we illustrate its performance and benchmark it against alternative frequentist DPA and DAA methods using data from 67 human gut microbiome studies.

Methods

Schematic illustration of differential prevalence analysis

The basic case of DPA, on which we focus in this paper, is illustrated in Figure 1. It involves comparing the observed presence/absence of taxonomic features between two groups, such as healthy and non-healthy subjects (referred to as “control” and “case”, respectively).

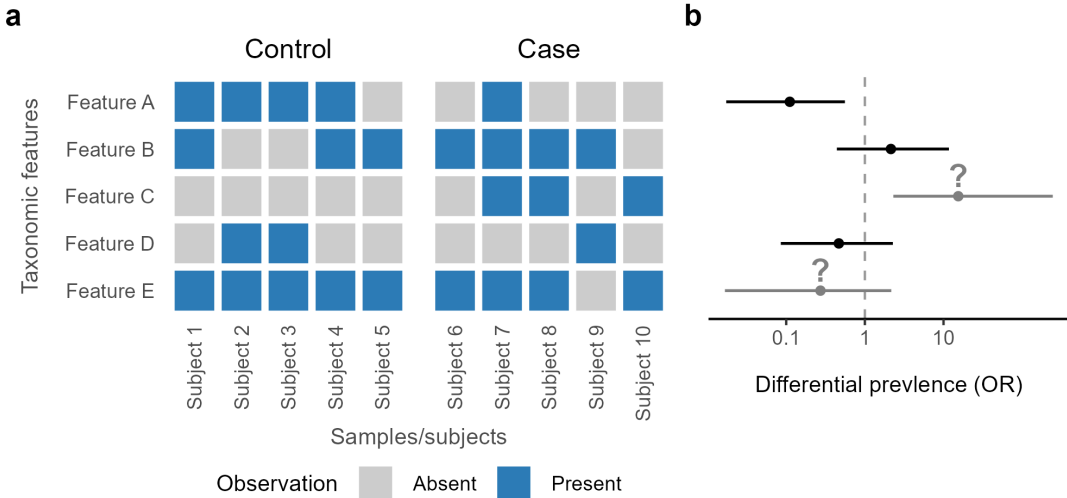


Figure 1: Schematic illustration of differential prevalence analysis. a) A presence/absence matrix for five taxonomic features (e.g., species or genera) across five control and five case subjects (samples). b) Results of DPA, i.e., the estimated differential prevalence effects with uncertainty intervals for the five features shown in a). The question marks indicate boundary cases (features C and E) where the prevalence is either 0% or 100% in one of the two groups. In such scenarios, some frequentist methods fail to yield finite point estimates, confidence intervals or p-values. OR = Odds ratio

DiPPER – A Bayesian hierarchical model for differential prevalence analysis

Here, we provide a detailed description of our method DiPPER. For clarity of exposition, we describe the model using a binary case/control setting, although the binary predictor can also be replaced with a standardized continuous variable.

Let y_{ij} denote the observed presence (1) or absence (0) of feature $j = 1, \dots, K$, in subject/sample $i = 1, \dots, N$. We model y_{ij} using a logistic regression framework where the probability of presence, p_{ij} , is defined as:

$$\log \left(\frac{p_{ij}}{1 - p_{ij}} \right) = \alpha_j + \beta_j \cdot \text{group}_i + \beta_j^{\text{reads}} \cdot \text{reads}_i + \sum_{m=1}^M \beta_j^{(m)} \cdot x_i^{(m)}. \quad (1)$$

Here, group_i is a binary indicator for the study group (0 = control, 1 = case), reads_i represents the centered \log_{10} -transformed total read count (sequencing depth), and $x_i^{(m)}$ represents the m -th additional covariate for sample i .

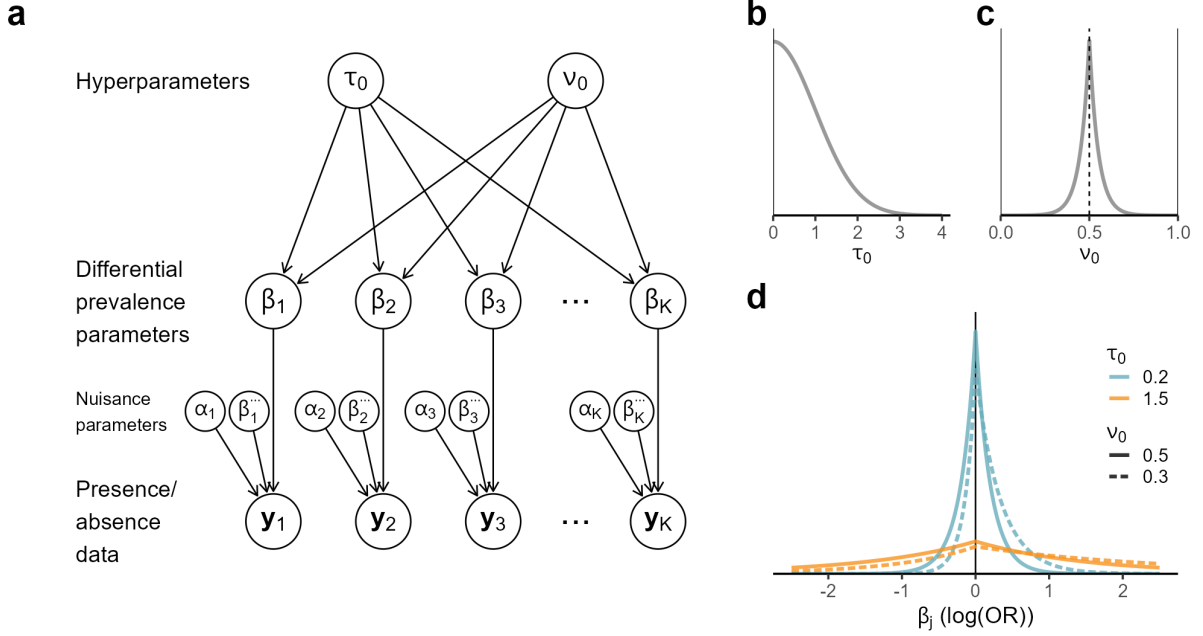


Figure 2: Structure of DiPPER. a) Directed acyclic graph of the model hierarchy. The hyperparameters τ_0 and v_0 determine the scale (width) and skewness of the prior for the differential prevalence parameters β_1, \dots, β_K . The nuisance parameters refer to intercepts (α_j) and regression coefficients for covariates ($\beta_j^{(m)}$), while $\mathbf{y}_1, \dots, \mathbf{y}_K$ indicate the observed presence/absence data vectors. b) The half-normal prior for the global scale τ_0 . c) The Laplace prior for the skewness parameter v_0 . d) The asymmetric Laplace prior for each parameter β_j under four illustrative combinations of τ_0 and v_0 . The index $j = 1, \dots, K$ indicates features.

The conditional distributions (see Figure 2) are specified as follows:

$$\tau_0 \sim \text{HalfNormal}(0, 1^2) \quad (2.1)$$

$$v_0 \sim \text{Laplace}(\mu_v = 0.50, \sigma_v = 0.05) \quad (2.2)$$

$$\beta_j | \tau_0, v_0 \sim \text{AsymmLaplace}(\mu_0 = 0, \tau_0, v_0) \quad (2.3)$$

$$\alpha_j \sim \mathcal{N}(0, 5^2) \quad (2.4)$$

$$\beta_j^{\text{reads}} \sim \mathcal{N}(2, 2^2) \quad (2.5)$$

$$\beta_j^{(m)} \sim \mathcal{N}(0, 1^2) \quad (2.6)$$

$$y_{ij} | p_{ij} \sim \text{Bernoulli}(p_{ij}) \quad (2.7)$$

The parameters of interest, β_j , each expressed as a log-odds ratio, quantify the differential prevalence of feature j between the case and control groups. All β_j parameters share a common asymmetric Laplace prior distribution (2.3, Figure 2d). This prior is peaked at zero ($\mu_0 = 0$), reflecting the assumption that most taxonomic features are not differentially prevalent. For feature-specific intercepts α_j , we utilize a weakly informative prior (2.4).

The hyperparameters τ_0 and v_0 determine the scale (width) and skewness of the asymmetric Laplace prior, respectively. The scale parameter τ_0 thus controls the overall degree of shrinkage of the β_j parameters towards zero. The half-normal hyperprior (2.1, Figure 2b) ensures the positivity and regularization of τ_0 . The skewness parameter v_0 determines the skewness of the asymmetric Laplace prior. Its hyperprior is centered at 0.50 (2.2, Figure 2c) to favor symmetry a priori. However, allowing v_0 to deviate from 0.50 accommodates our observation from microbiome studies that differentially prevalent features often share the same direction of effect

within a study (see Supplementary Figure 6).

Moreover, since sequencing depth can affect the probability of detecting a taxonomic feature [3], the centered \log_{10} -transformed total read count is included as a covariate in the model. We employ a moderately informative prior for β_j^{reads} (2.5), reflecting the expectation that a higher sequencing depth increases the probability of detecting a feature. The \log_{10} -transformation and the prior mean of 2 were selected based on our empirical observations.

Lastly, variables $x_i^{(m)}$ ($m = 1, \dots, M$) represent M additional covariates, such as age, body-mass index, and sex, that are potential confounders but not of interest themselves. These should be supplied as binary indicators or standardized continuous variables. For the regression coefficients $\beta_j^{(m)}$ of these variables, a weakly informative prior $N(0, 1^2)$ is employed.

Posterior sampling

Posterior sampling was performed using the No-U-Turn Sampler in Stan [12] (4 chains, 3,000 iterations, 1,000 warmup), yielding a total of 8,000 posterior samples. Convergence was confirmed in all datasets, indicated by the potential scale reduction factor $\hat{R} < 1.02$ for all parameters of interest and an absence of divergent transitions.

Performance evaluation and benchmarking

Original datasets

We evaluated the performance of DiPPER and alternative methods using data from 67 published human gut microbiome studies, employing 16S rRNA gene sequencing (16S) or shotgun metagenomic sequencing (shotgun) [13, 14]. These studies compared healthy individuals to those with various diseases, such as colorectal cancer (CRC), inflammatory bowel disease (IBD), and type 1 or type 2 diabetes, or other conditions such as obesity. As some studies included multiple non-healthy groups, the total number of datasets extracted from the 67 studies was 80 (39 16S and 41 shotgun datasets).

Sample sizes in the datasets ranged from 20 to 747. The 16S and shotgun datasets were analyzed at the genus and species levels, respectively. Features present in fewer than four samples were filtered out. Following filtering, the number of features ranged from 49 to 495 per dataset. Detailed descriptions of the datasets are provided in the Supplementary Material.

Definition of statistical significance

For frequentist methods, statistical significance at level α was defined as an FDR-adjusted p-value $q < \alpha$. We applied the standard Benjamini-Hochberg procedure [15] to calculate FDR-adjusted p-values, except for LDM-DP (see below), which uses an internal permutation-based approach.

To benchmark DiPPER against frequentist methods, we defined an analogous criterion for statistical significance. For DiPPER, the DPA result for a feature was considered “significant” if its $(1 - \alpha) \times 100\%$ equal-tailed credible interval (defined by the $\alpha/2$ and $1 - \alpha/2$ posterior quantiles) excluded zero.

Throughout this study, we employed a significance level of $\alpha = 0.10$ unless otherwise stated. This threshold was chosen to ensure a sufficient number of significant findings, thereby enabling a robust estimation of our performance metrics. We note, however, that using the conventional $\alpha = 0.05$ would not substantially alter our conclusions (see Supplementary Figures 10 and 11).

Performance metrics

Null data error rate We estimated the empirical error rate of our and seven alternative methods using 480 null datasets where no true differences between the groups existed. These datasets were constructed by performing 10 random case-control splits within the healthy groups of the 48 studies (out of 67) that contained at least 20 healthy subjects. We used the proportion of null datasets with *any* significant findings (λ) as our error rate metric. Theoretically, for a method that controls the FDR at level α , this error rate (λ) is expected to be at or below α under the global null hypothesis (for details, see Supplementary Material).

Number of significant findings To assess the sensitivity to detect potentially differentially prevalent features, we calculated the total number of significant findings produced by each method across the 80 original datasets. While a high number of findings may indicate high statistical power, it can also reflect an inflated false positive rate. This metric must therefore be evaluated alongside the null data error rate.

Cross-study replicability While a significant finding in a single study does not necessarily indicate a true association, identifying the same taxonomic feature as differentially prevalent in the same direction in another independent study investigating the same condition suggests a true biological signal. Conversely, if a significant association is found for a feature in two studies but with opposite directions, it is likely a false positive result in at least one of them. We thus used the number of replicated and conflicting findings as additional proxies for power and error rate. We evaluated replication using 110 pairs of datasets that investigated the same disease and employed the same sequencing method (16S or shotgun; for details, see Supplementary Material).

Compared methods

We benchmarked the performance of DiPPER against seven different DPA or DAA methods. A summary of these methods is presented in Table 1.

Table 1: Methods included in the benchmark comparison with DiPPER

Method	Type	Description
Wald	DPA	Logistic regression, Wald test
LRT	DPA	Logistic regression, likelihood ratio test
Firth [9]	DPA	Logistic regression, penalized likelihood ratio test
MaAsLin3-DP [4]	DPA	Logistic regression, data augmentation + Wald test
LDM-DP [8]	DPA	F-tests with rarefaction, permutation-based multiplicity adjustment
MaAsLin2 [16]	DAA	Linear model, log-transformed relative abundances
LinDA [17]	DAA	Linear model, CLR-transformation + bias correction

DPA = differential prevalence analysis; DAA = differential abundance analysis.

First, we included three versions of frequentist logistic regression. These methods share an identical likelihood formulation with DiPPER (Equations 1 and 2.7) but differ in how p-values are calculated: the Wald test (referred to as Wald), the standard likelihood ratio test (LRT), or the likelihood ratio test based on Firth's penalized likelihood (Firth) [9].

Additionally, we benchmarked DiPPER against two methods specifically designed for microbial DPA. The first is the DPA component of the recently published MaAsLin3 DAA method (MaAsLin3-DP) [4]. It employs logistic regression, controls for total read counts, and calculates p-values using the Wald test combined with data augmentation. The second is the DPA method from the LDM package (LDM-DP) [8], which utilizes rarefaction combined with F-tests and accounts for multiplicity via a permutation-based approach. Since LDM-DP does not provide differential prevalence estimates, we supplemented it with point estimates from Firth in the cross-study replication analysis.

Finally, to benchmark DiPPER against DAA, we included two representative methods. As a simple baseline method, we selected MaAsLin2 [16], which fits linear models to log-transformed relative abundances. Despite its simplicity, MaAsLin2 has performed well in recent method benchmarks [5, 18]. As a state-of-the-art method that explicitly models compositional effects, we used LinDA [17], which applies linear models with bias correction to centered log-ratio (CLR) transformed abundances. In the context of our study, a practical advantage of LinDA compared to several other state-of-the-art methods is that it accepts relative abundances as input, thus avoiding the need to use approximated counts for the shotgun datasets obtained from the *curatedMetagenomicData* package [14].

Results

Illustrative examples

Before quantitatively evaluating the performance of DiPPER, we visually illustrate its performance with two examples by comparing differential prevalence estimates and 90% credible intervals provided by DiPPER against frequentist results (Figure 3). To specifically demonstrate how DiPPER addresses issues typical of frequentist DPA, we chose maximum likelihood estimates and 90% confidence intervals (CIs), based on the Wald approximation, to represent frequentist results. To demonstrate the impact of adjusting for multiple testing, we applied the Bonferroni correction to CIs. Although the full datasets in the two examples comprised 312 and 171 species, for clarity of illustration, we present results only for the first 25 species in alphabetical order.

Our first example (Figure 3a) demonstrates the performance of DiPPER on a null dataset, where 61 healthy individuals from a gut microbiome study [19] were randomly assigned to “case” ($N = 31$) and “control” ($N = 30$) groups. As shown in the figure, the median posterior estimates provided by DiPPER are very close to the true parameter value of one ($OR = 1$). In contrast, the corresponding frequentist estimates show substantial variation. Furthermore, the 90% credible intervals from DiPPER consistently include the null value 1, unlike the unadjusted frequentist 90% CIs, which exclude it in three cases (highlighted in orange). Notably, the credible intervals from DiPPER are considerably narrower than the frequentist CIs. Lastly, while the Bonferroni adjustment extends the CIs to include one, thereby effectively eliminating the false positives, it also makes the CIs excessively wide, thereby reducing estimation precision.

In our second example (Figure 3b), we analyzed data from a study comparing Indian subjects with and without colorectal cancer (CRC, $N = 30$ in each group) [20]. This represents a scenario in which a significant portion of species is expected to truly differ in prevalence between the groups. Here, the posterior estimates provided by DiPPER closely align with the frequentist ML estimates. Moreover, the 90% credible intervals from DiPPER are similar to the unadjusted 90% CIs but notably narrower than the Bonferroni-adjusted CIs. Crucially, all species identified as differentially prevalent by the unadjusted frequentist approach are also detected by DiPPER. In contrast, applying the Bonferroni correction results in many potentially

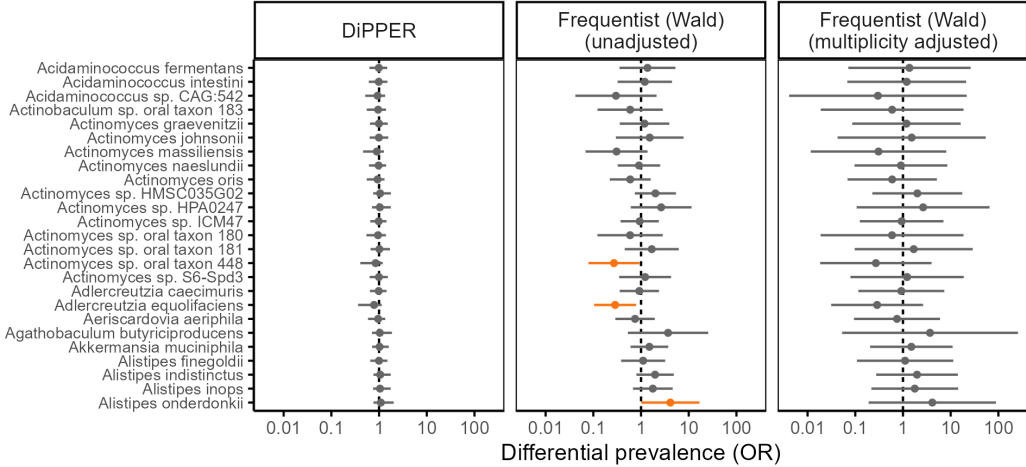
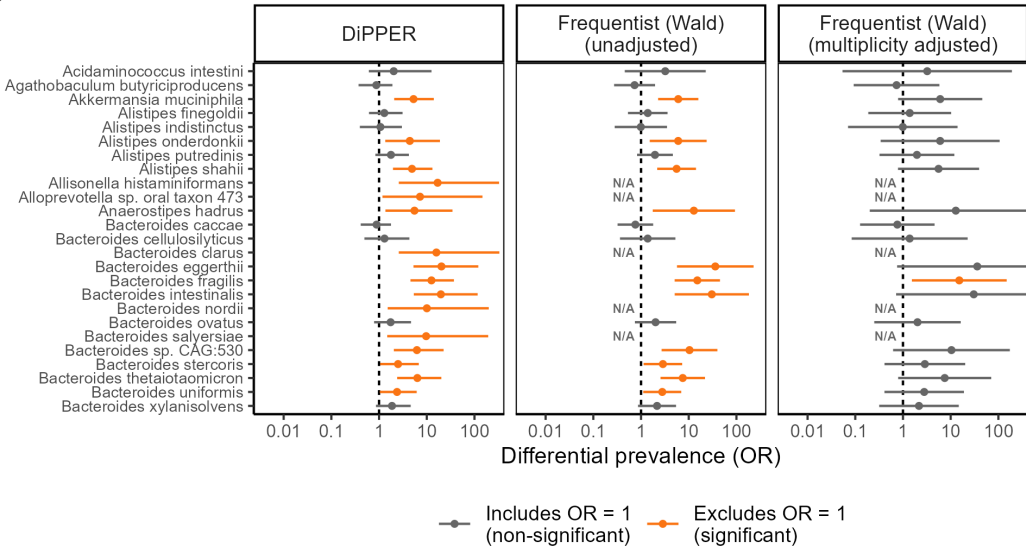
a**b**

Figure 3: Illustration of DiPPER performance and comparison with frequentist logistic regression (Wald). a) DPA results for 25 species (the first 25 in alphabetical order) in a null dataset where “case” and “control” groups ($N = 31$ and 30) were randomly assigned among healthy subjects in a gut microbiome study [19]. b) Results for 25 species in a dataset comparing healthy subjects ($N = 30$) and subjects with CRC ($N = 30$) [20]. In both panels, the points indicate the median posterior (DiPPER) or maximum likelihood (frequentist) differential prevalence estimates. The error bars represent 90% credible intervals (left), unadjusted 90% CIs (middle), or Bonferroni-adjusted 90% CIs based on the Wald approximation (right). N/A indicates a non-finite result.

differentially prevalent features going undetected.

Importantly, the second example also includes five boundary cases where the prevalence of a species is either 0% or 100% in one of the comparison groups. While DiPPER identifies these species as differentially prevalent, the frequentist approaches fail to provide finite estimates for them (labeled ‘N/A’ in Figure 3b), thus effectively omitting these potentially relevant species.

Null data error rate

For DiPPER, the null data error rate (the proportion of the 480 null datasets with any significant features, λ), was approximately at the nominal level of 0.10 (Figure 4a). In contrast, among the frequentist DPA methods, the error rates were substantially below the nominal level for both Wald ($\lambda = 0.02$) and MaAsLin3-DP ($\lambda = 0.03$), and slightly below the nominal level for Firth and LDM-DP (both $\lambda = 0.07$). However, LRT had a considerably higher error rate ($\lambda = 0.19$). Among the DAA methods, the error rate of MaAsLin2 was at the nominal level at $\lambda = 0.10$, whereas LinDA had its error rate somewhat above the nominal level at $\lambda = 0.14$.

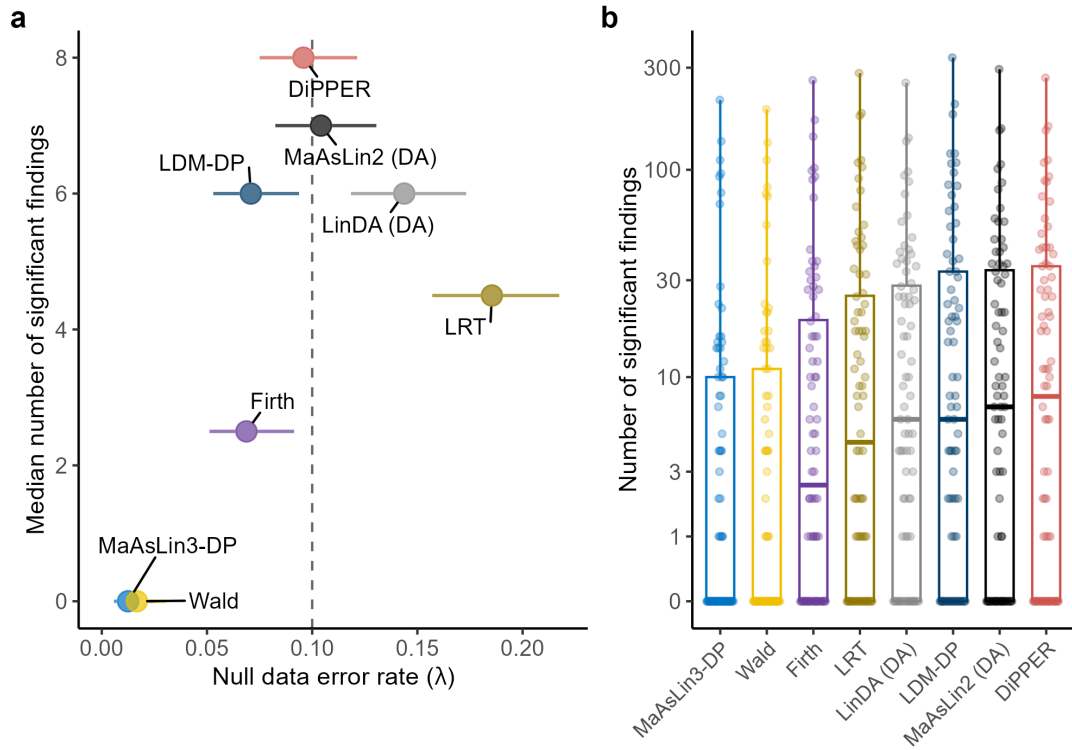


Figure 4: Performance of DiPPER and competing frequentist DPA and DAA methods on 480 null datasets and on 80 original datasets. a) x-axis: Null data error rate (λ), defined as the proportion of the 480 null datasets in which any significant findings were made. Ideally, this proportion should be at or below the significance level $\alpha = 0.10$ (vertical dashed line). The error bars indicate 90% confidence intervals for the error rate estimates. y-axis: Median number of significant findings across the 80 original datasets. b) The number of significant findings in each of the 80 original datasets. Note the logarithmic scale. The methods are ordered by the median number of significant findings.

Number of significant findings

The number of significant findings detected by each method across the 80 original datasets is presented in Figure 4b. On average, the highest number of associations was detected by LDM-DP (mean = 29.2; median = 6.0), DiPPER (26.1; 8.0), and MaAsLin2 (24.8; 7.0). Slightly fewer findings were obtained with LRT (24.7; 4.5) and LinDA (22.9; 6.0), followed by Firth (20.1; 2.5). The least sensitive methods were MaAsLin3-DP (13.5; 0.0) and Wald (13.0; 0.0), which failed to detect any differentially prevalent features in more than half of the datasets.

Given that the total number of features varies substantially across datasets, we also evaluated the *proportion* of features identified as significant in each dataset. However, the relative

sensitivity of the methods remained consistent with this alternative metric (Supplementary Figure 7).

Cross-study replicability

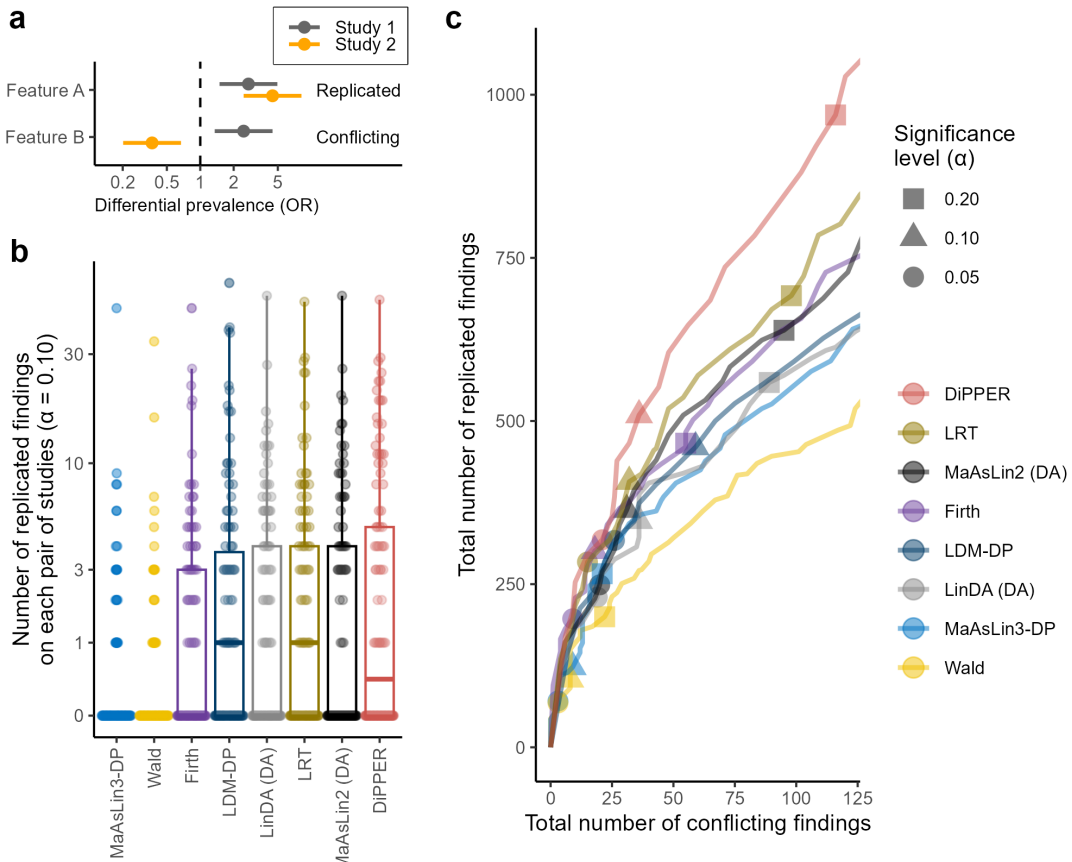


Figure 5: Replication of DPA and DAA results across studies. Replication was evaluated in 110 pairs of datasets, with each pair consisting of datasets from studies examining the same disease and utilizing the same sequencing methods (either 16S or shotgun). a) The definition of replicated and conflicting results. b) The number of replicated results across the study pairs (significance level $\alpha = 0.10$). The methods are ordered by the 75% quantile of the number of replicated findings. c) The total number of replicated results plotted against the total number of conflicting results at varying significance levels.

For each method evaluated, the number of replicated findings across the 110 pairs of independent datasets is shown in Figure 5b. Given that 45 of the 110 study pairs yielded no replicated findings, we employ the 75% quantile (Q75) as the second summary statistic. On average, DiPPER yielded the highest number of replicated findings (mean = 4.6; Q75 = 5.0). It was followed by LDM-DP supplemented with estimates from Firth (4.2; 3.8), LRT (3.7; 4.0), the DAA methods MaAsLin2 (3.3; 4.0) and LinDA (3.2; 4.0), and the DPA method Firth (2.7; 3.0). The lowest numbers of replicated findings were observed for MaAsLin3-DP (1.1; 0.0) and Wald (0.8; 0.0).

Figure 5c plots the total number of replicated findings with respect to the total number of conflicting findings across varying significance levels. It demonstrates that DiPPER consistently outperformed the competing methods.

Robustness to hyperprior specifications

We evaluated the robustness of DiPPER to the hyperprior specifications for τ_0 and ν_0 (Equations 2.1 and 2.2). Altering the prior for the scale parameter τ_0 had a negligible effect on performance (see Supplementary Figures 8 and 9). Allowing the skewness parameter ν_0 to vary more freely than in our default choice (Equation 2.2, Figure 2c) yielded a slightly elevated null data error rate ($\lambda = 0.13$) but did not affect other performance metrics.

In contrast, enforcing symmetry on the asymmetric Laplace prior by fixing $\nu_0 = 0.50$ yielded more conservative performance, reducing both the null data error rate ($\lambda = 0.05$) and the number of significant findings in the original datasets (mean = 24.7; median = 4.5). This variant of the method may serve as a preferable alternative in scenarios where asymmetric prevalence differences are not expected.

Adaptation to differential abundance analysis

We also explored the applicability of the Bayesian hierarchical approach from DiPPER to DAA. To this end, we developed a Bayesian adaptation of MaAsLin2. This method retains the identical prior and hyperprior structure as DiPPER (Equations 2.1–2.6) but replaces the binomial likelihood with a Gaussian likelihood to analyze standardized log-transformed relative abundances (for details, see Supplementary Material).

The preliminary results were encouraging (Supplementary Figures 8 and 9). The Bayesian version of MaAsLin2 demonstrated a good null data error rate ($\lambda = 0.08$) while exhibiting sensitivity superior to other methods (mean = 28.8, median = 13.0 findings in the original datasets). Furthermore, its ratio of replicated to conflicting findings was comparable to that of DiPPER. However, we caution that this apparent performance gain may partially reflect the amplification of compositional artifacts due to the allowed asymmetry of the prior. Consequently, further validation is warranted before its wider adoption in DAA.

Discussion

We have demonstrated how analyzing presence/absence data with a Bayesian hierarchical model enables effective detection of disease-associated taxonomic features while producing easily interpretable effect size estimates and uncertainty intervals that are inherently adjusted for multiplicity. Specifically, using empirical data from dozens of human gut microbiome studies, we demonstrated that our method, DiPPER, outperformed alternative frequentist differential prevalence and abundance methods.

We have also shown that different frequentist methods yield surprisingly discordant results in microbial DPA. For instance, there was over a two-fold difference in the total number of significant findings detected between the least and most sensitive methods. Regarding the performance of individual methods, logistic regression based on the Wald test cannot be recommended for DPA as it fails to provide results in boundary cases. The method based on the standard likelihood ratio test (LRT) is also problematic due to its high error rate. A reliable, albeit conservative, option is provided by the differential prevalence method within the MaAsLin3 package [4]. The penalized likelihood method (Firth) offers robust performance with decent sensitivity and good error rate control. Lastly, the differential prevalence method from the LDM package [8] yields high sensitivity and robust error rate control, but it does not provide estimates of differential prevalence, which is an important practical limitation.

A plausible explanation for the favorable performance of DiPPER against other DPA methods is that the asymmetric Laplace distribution (2.3) effectively approximates the distribution

of true prevalence differences between the study groups. Specifically, the chosen prior accommodates our empirical observation that within a study, prevalence differences are rarely symmetrically distributed; instead, differentially prevalent taxonomic features often share the same direction (see Supplementary Figure 6).

The use of a common prior distribution to borrow information across features is not unique to DiPPER, but aligns with well-established practices in high-throughput data analysis. For example, it has previously been employed in popular differential gene expression tools to stabilize variance estimates via empirical Bayes techniques [21, 22, 23]. Moreover, while fully Bayesian hierarchical methods for effect size estimation also exist [24, 25, 26], these typically differ from our approach by concentrating on calculating posterior probabilities for null hypotheses, for instance, by employing spike-and-slab priors [26, 27], and using separate adjustments to control the FDR [28]. To the best of our knowledge, DiPPER is thus the first high-throughput data analysis method to employ estimation-based feature detection with a Laplace-type prior at its core.

Our observation that DiPPER outperformed the compared DAA methods reinforces recent reports in which using presence/absence data alone maintained classification accuracy [1, 2]. These results suggest that associations between taxonomic features and the studied conditions may be primarily driven by the presence of the features, rather than their abundance. In addition, the abundances may exhibit substantial stochastic variation that obscures the biological signal, whereas binary presence/absence data can offer a more robust signal-to-noise ratio. Although finite sequencing depth affects detection sensitivity [3], the successful replication of prevalence differences across studies with widely varying sequencing depths suggests these differences have a biological origin rather than being mere artifacts of sequencing limitations.

The main strength of our study lies in the use of numerous real datasets, which provide strong empirical evidence for DiPPER's performance. Moreover, the primary motivation for the method stems from empirical observations, rather than a mechanistically grounded model of the biological processes generating the data. While this limited theoretical basis could be seen as a limitation, it also presents a strength: the lack of rigid process-specific assumptions makes the model potentially applicable to other high-throughput profiling studies. Nevertheless, despite its favorable performance, a notable practical drawback of DiPPER is its long runtime due to the computationally demanding MCMC sampling process. For the analyzed datasets, execution times ranged from 2 minutes to a few hours on a standard laptop. However, optimization of MCMC techniques and feature filtering could mitigate this issue.

Regarding future research, our additional analysis suggests that DiPPER's hierarchical modeling approach could be extended to differential abundance analysis. Furthermore, while DiPPER was motivated by empirical observations from microbiome studies, it may be applicable to other omics data, such as transcriptomics, proteomics, metabolomics, and single-cell data. However, such applications warrant further investigation given the technical and biological differences across research domains.

Key points

- We introduced DiPPER, a novel Bayesian hierarchical model for differential prevalence analysis.
- The method outperformed alternative differential prevalence and abundance methods in microbiome data by combining high sensitivity with effective error control.
- Frequentist alternatives yielded highly discordant results, with over a two-fold difference in the number of detected taxonomic features.
- DiPPER provides differential prevalence estimates and uncertainty intervals that are inherently adjusted for multiplicity.
- Bayesian hierarchical modeling can offer a favorable alternative to inference based on multiplicity-adjusted p-values.

Competing interests

The authors declare that they have no competing interests.

Author contributions

JP conceived the idea, carried out the analyses and drafted the manuscript. KA, JK and LL supervised JP and participated in editing and reviewing the manuscript. LL acquired the funding. The authors read and approved the final manuscript.

Acknowledgments

This work was supported by Strategic Research Council established within the Research Council of Finland (decision 372345 to LL, JP). The authors wish to acknowledge CSC – IT Center for Science, Finland, for computational resources.

Data availability

An example workflow, the processed datasets, and the analysis source code are available at <https://github.com/jepelt/differential-prevalence>. The raw data were sourced from the MicrobiomeHD database [13] and the curatedMetagenomicData (version 3.14.0) R package [14]. All data analyses were performed in R 4.4.2 [29].

To further facilitate the use of DiPPER, we are currently integrating it into our microbiome data science framework in R/Bioconductor [30], a widely used research software repository for computational life science research and education [31].

References

- [1] Renato Giliberti, Sara Cavalieri, Italia Elisa Mauro, Danilo Ercolini, and Edoardo Pasolli. Host phenotype classification from human microbiome data is mainly driven by the presence of microbial taxa. *PLoS computational biology*, 18(4), 4 2022.
- [2] Zuzanna Karwowska, Oliver Aasmets, Tõnu Esko, Lili Milani, Andres Metspalu, Mait Metspalu, Tomasz Kosciolek, and Elin Org. Effects of data transformation and model selection on feature importance in microbiome classification data. *Microbiome*, 13(1):1–14, 12 2025.
- [3] Jacob T. Barlow, Said R. Bogatyrev, and Rustem F. Ismagilov. A quantitative sequencing framework for absolute abundance measurements of mucosal and luminal microbial communities. *Nature Communications* 2020 11:1, 11(1):1–13, 5 2020.
- [4] William A. Nickols, Thomas Kuntz, Jiaxian Shen, Sagun Maharjan, Himel Mallick, Eric A. Franzosa, Kelsey N. Thompson, Jacob T. Nearing, and Curtis Huttenhower. MaAsLin 3: refining and extending generalized multivariable linear models for meta-omic association discovery. *Nature Methods* 2026, pages 1–11, 1 2026.
- [5] Juho Pelto, Kari Auranen, Janne V Kujala, and Leo Lahti. Elementary methods provide more replicable results in microbial differential abundance analysis. *Briefings in Bioinformatics*, 26(2):130, 3 2025.
- [6] Gregory B. Gloor, Jean M. Macklaim, Vera Pawlowsky-Glahn, and Juan J. Egozcue. Microbiome Datasets Are Compositional: And This Is Not Optional. *Frontiers in microbiology*, 8(NOV), 11 2017.
- [7] Michael R McLaren, Amy D Willis, and Benjamin J Callahan. Consistent and correctable bias in metagenomic sequencing experiments. *eLife*, 8, 9 2019.
- [8] Yi Juan Hu, Andrea Lane, and Glen A. Satten. A rarefaction-based extension of the LDM for testing presence–absence associations in the microbiome. *Bioinformatics*, 37(12):1652, 6 2021.
- [9] David Firth. Bias Reduction of Maximum Likelihood Estimates. *Biometrika*, 80(1):27, 3 1993.
- [10] Andrew Gelman, Jennifer Hill, and Masanao Yajima. Why We (Usually) Don’t Have to Worry About Multiple Comparisons. *Journal of Research on Educational Effectiveness*, 5(2):189–211, 4 2012.
- [11] Arvid Sjölander and Stijn Vansteelandt. Frequentist versus Bayesian approaches to multiple testing. *European Journal of Epidemiology*, 34:809–821, 2019.
- [12] Bob Carpenter, Andrew Gelman, Matthew D. Hoffman, Daniel Lee, Ben Goodrich, Michael Betancourt, Marcus A. Brubaker, Jiqiang Guo, Peter Li, and Allen Riddell. Stan: A Probabilistic Programming Language. *Journal of Statistical Software*, 76(1):1–32, 1 2017.
- [13] Claire Duvallet, Sean M. Gibbons, Thomas Gurry, Rafael A. Irizarry, and Eric J. Alm. Meta-analysis of gut microbiome studies identifies disease-specific and shared responses. *Nature Communications*, 8(1):1784, 12 2017.

[14] Edoardo Pasolli, Lucas Schiffer, Paolo Manghi, Audrey Renson, Valerie Obenchain, Duy Tin Truong, Francesco Beghini, Faizan Malik, Marcel Ramos, Jennifer B. Dowd, Curtis Huttenhower, Martin Morgan, Nicola Segata, and Levi Waldron. Accessible, curated metagenomic data through ExperimentHub. *Nature Methods* 2017 14:11, 14(11):1023–1024, 10 2017.

[15] Yoav Benjamini and Yosef Hochberg. Controlling the False Discovery Rate: A Practical and Powerful Approach to Multiple Testing. *Journal of the Royal Statistical Society: Series B (Methodological)*, 57(1):289–300, 1 1995.

[16] Himel Mallick, Ali Rahnavard, Lauren J. McIver, Siyuan Ma, Yancong Zhang, Long H. Nguyen, Timothy L. Tickle, George Weingart, Boyu Ren, Emma H. Schwager, Suvo Chatterjee, Kelsey N. Thompson, Jeremy E. Wilkinson, Ayshwarya Subramanian, Yiren Lu, Levi Waldron, Joseph N. Paulson, Eric A. Franzosa, Hector Corrada Bravo, and Curtis Huttenhower. Multivariable association discovery in population-scale meta-omics studies. *PLOS Computational Biology*, 17(11):e1009442, 11 2021.

[17] Huijuan Zhou, Kejun He, Jun Chen, and Xianyang Zhang. LinDA: linear models for differential abundance analysis of microbiome compositional data. *Genome Biology*, 23(1):95, 12 2022.

[18] Jakob Wirbel, Morgan Essex, Sofia Kirke Forslund, and Georg Zeller. A realistic benchmark for differential abundance testing and confounder adjustment in human microbiome studies. *Genome Biology* 2024 25:1, 25(1):1–26, 9 2024.

[19] Georg Zeller, Julien Tap, Anita Y Voigt, Shinichi Sunagawa, Jens Roat Kultima, Paul I Costea, Aurélien Amiot, Jürgen Böhm, Francesco Brunetti, Nina Habermann, Rajna Hercog, Moritz Koch, Alain Luciani, Daniel R Mende, Martin A Schneider, Petra Schrotz-King, Christophe Tournigand, Jeanne Tran Van Nhieu, Takuji Yamada, Jürgen Zimmermann, Vladimir Benes, Matthias Kloos, Cornelia M Ulrich, Magnus von Knebel Doeberitz, Iradj Sobhani, and Peer Bork. Potential of fecal microbiota for early-stage detection of colorectal cancer. *Molecular systems biology*, 10(11):766, 11 2014.

[20] Ankit Gupta, Darshan B. Dhakan, Abhijit Maji, Rituja Saxena, Vishnu Prasoodanan P.K., Shruti Mahajan, Joby Pulikkan, Jacob Kurian, Andres M. Gomez, Joy Scaria, Katherine R. Amato, Ashok K. Sharma, and Vineet K. Sharma. Association of Flavonifractor plautii, a Flavonoid-Degrading Bacterium, with the Gut Microbiome of Colorectal Cancer Patients in India. *mSystems*, 4(6), 12 2019.

[21] Mark D Robinson, Davis J McCarthy, and Gordon K Smyth. edgeR: a Bioconductor package for differential expression analysis of digital gene expression data. *Bioinformatics (Oxford, England)*, 26(1):139–40, 1 2010.

[22] Michael I Love, Wolfgang Huber, and Simon Anders. Moderated estimation of fold change and dispersion for RNA-seq data with DESeq2. *Genome biology*, 15(12):550, 2014.

[23] Matthew E Ritchie, Belinda Phipson, Di Wu, Yifang Hu, Charity W Law, Wei Shi, and Gordon K Smyth. limma powers differential expression analyses for RNA-sequencing and microarray studies. *Nucleic acids research*, 43(7):e47, 4 2015.

[24] Will Landau, Jarad Niemi, and Dan Nettleton. Fully Bayesian analysis of RNA-seq counts for the detection of gene expression heterosis. *Journal of the American Statistical Association*, 114(526):610, 4 2018.

- [25] Ran Bi and Peng Liu. A semi-parametric Bayesian approach for detection of gene expression heterosis with RNA-seq data. *Journal of Applied Statistics*, 50(1):214, 2021.
- [26] M. Büttner, J. Ostner, C. L. Müller, F. J. Theis, and B. Schubert. scCODA is a Bayesian model for compositional single-cell data analysis. *Nature Communications* 2021 12:1, 12(1):6876–, 11 2021.
- [27] W. Thomson, S. Jabbari, A. E. Taylor, W. Arlt, and D. J. Smith. Simultaneous parameter estimation and variable selection via the logit-normal continuous analogue of the spike-and-slab prior. *Journal of the Royal Society Interface*, 16(150):20180572, 1 2019.
- [28] Michael A. Newton, Amine Noueiry, Deepayan Sarkar, and Paul Ahlquist. Detecting differential gene expression with a semiparametric hierarchical mixture method. *Biostatistics*, 5(2):155–176, 4 2004.
- [29] R Core Team. R: A Language and Environment for Statistical Computing, 2024.
- [30] Tuomas Borman, Giulio Benedetti, Geraldson Muluh, Aura Raulo, Benjamin Valderrama, Artur Sannikov, Stefanie Peschel, Yihan Liu, Rasmus Hindström, OMA consortium, Katariina Pärnänen, Christian L. Müller, Aki S. Havulinna, Sudarshan Shetty, Marcel Ramos, Domenick J. Braccia, Héctor Corrada Bravo, Felix M. Ernst, Levi Waldron, Thomaz F. S. Bastiaanssen, Himel Mallick, and Leo Lahti. Orchestrating Microbiome Analysis with Bioconductor. *bioRxiv*, page 2025.10.29.685036, 10 2025.
- [31] Jenny Drnevich, Frederick J. Tan, Fabricio Almeida-Silva, Robert Castelo, Aedin C. Culhane, Sean Davis, Maria A. Doyle, Ludwig Geistlinger, Andrew R. Ghazi, Susan Holmes, Leo Lahti, Alexandru Mahmoud, Kozo Nishida, Marcel Ramos, Kevin Rue-Albrecht, David J. H. Shih, Laurent Gatto, and Charlotte Soneson. Learning and teaching biological data science in the Bioconductor community. *PLoS computational biology*, 21(4), 3 2025.

Supplementary material

Directional imbalance of differentially prevalent taxonomic features

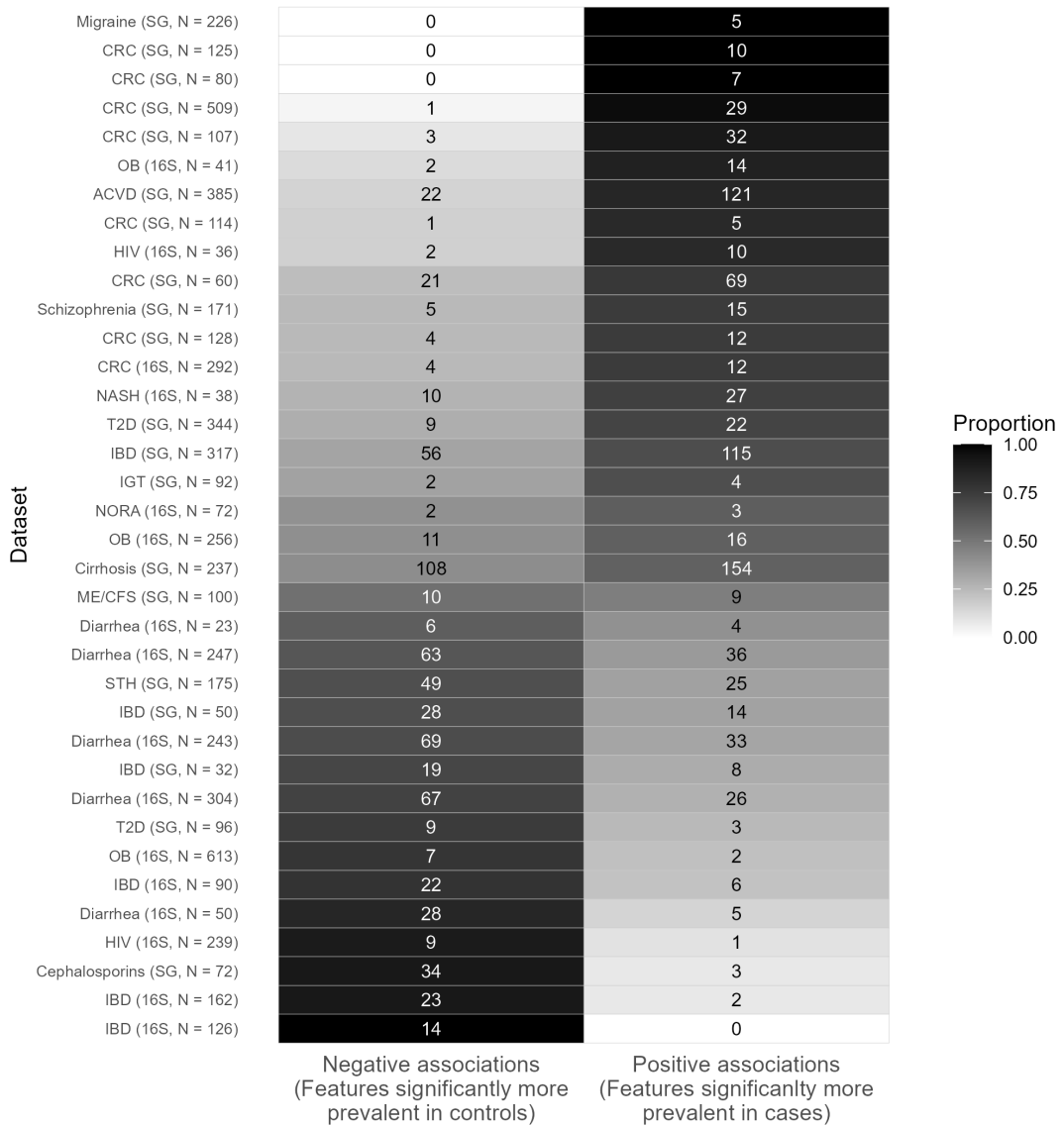


Figure 6: Directional imbalance of differentially prevalent taxonomic features within studies. The heatmap displays the count (numbers) and proportion (color gradient) of differentially prevalent features (identified by Firth, $FDR < 0.10$). Only the datasets (out of 80) with ≥ 5 significant findings are included. Row labels indicate studied disease, sequencing type, and sample size (N). The figure illustrates that significant findings within individual studies typically display a strong directional imbalance, with most significant features being either more prevalent in cases or more prevalent in controls. This observation motivates the use of the asymmetric Laplace prior in DiPPER.

Original datasets

Table 2: The original 16S rRNA gene sequencing datasets used in the study.

Dataset ID	Condition	Seq.	N (Case)	N (Control)
asd_son	ASD	16S	59	44
autism_kb	ASD	16S	19	20
cdi_schubert_cdi	Diarrhea (CDI)	16S	93	154
cdi_schubert_diarrhea	Diarrhea	16S	89	154
cdi_vincent_v3v5	Diarrhea (CDI)	16S	25	25
cdi_youngster	Diarrhea	16S	19	4
crc_baxter_adenoma	Adenoma	16S	198	172
crc_baxter_crc	CRC	16S	120	172
crc_xiang	CRC	16S	21	22
crc_zackular_CRC	CRC	16S	30	30
crc_zackular_adenoma	Adenoma	16S	30	30
crc_zeller	CRC	16S	41	75
crc_zhao	CRC	16S	19	20
edd_singh	Diarrhea	16S	222	82
hiv_dinh	HIV	16S	21	15
hiv_lozupone	HIV	16S	23	13
hiv_noguerajulian	HIV	16S	205	34
ibd_alm	IBD	16S	66	24
ibd_engstrand_maxee	IBD	16S	45	35
ibd_gevers_2014	IBD	16S	146	16
ibd_huttenhower	IBD	16S	108	18
mhe_zhang_CIRR	Cirrhosis	16S	23	24
mhe_zhang_MHE	MHE	16S	18	24
nash_chan	NASH	16S	16	22
nash_ob_baker_NASH	NASH	16S	22	16
nash_ob_baker_OB	Obesity	16S	25	16
ob_goodrich_OB	Obesity	16S	185	428
ob_goodrich_OW	Overweight	16S	319	428
ob_gordon_2008_v2_OB	Obesity	16S	195	61
ob_gordon_2008_v2_OW	Overweight	16S	24	61
ob_ross_OB	Obesity	16S	37	6
ob_ross_OW	Overweight	16S	20	6
ob_zupancic	Obesity	16S	104	100
par_scheperjans	PD	16S	74	74
ra_littman_CRA	CRA	16S	26	28
ra_littman_NORA	NORA	16S	44	28
ra_littman_PSA	PSA	16S	16	28
t1d_alkanani	T1D	16S	57	55
t1d_mejialeon	T1D	16S	21	8

Abbreviations: ASD = autism spectrum disorder; CDI = *Clostridioides difficile* infection; CRA = chronic rheumatoid arthritis; CRC = colorectal cancer; IBD = inflammatory bowel disease; MHE = minimal hepatic encephalopathy; NASH = nonalcoholic steatohepatitis; NORA = new-onset rheumatoid arthritis; PD = Parkinson's disease; PSA = psoriatic arthritis; T1D = type 1 diabetes.

Table 3: The original shotgun metagenomic sequencing datasets used in the study.

Dataset ID	Condition	Seq.	N (Case)	N (Control)
BedarfJR_2017	PD	Shotgun	31	28
FengQ_2015_CRC	CRC	Shotgun	46	61
FengQ_2015_adenoma	Adenoma	Shotgun	47	61
GuptaA_2019	CRC	Shotgun	30	30
HMP_2019_ibdmdb	IBD	Shotgun	103	27
HallAB_2017	IBD	Shotgun	20	12
HanniganGD_2017_CRC	CRC	Shotgun	27	28
HanniganGD_2017_adenoma	Adenoma	Shotgun	26	28
Heitz-BuschartA_2016	T1D	Shotgun	10	10
IjazUZ_2017	IBD	Shotgun	12	38
JieZ_2017	ACVD	Shotgun	214	171
KarlssonFH_2013_IGT	IGT	Shotgun	49	43
KarlssonFH_2013_T2D	T2D	Shotgun	53	43
Lij_2014_IBD	IBD	Shotgun	129	10
Lij_2014_T1D	T1D	Shotgun	31	10
Lij_2014_T2D	T2D	Shotgun	79	10
Lij_2017_hypertension	Hypertension	Shotgun	99	41
Lij_2017_pre-hypertension	Pre-hypertension	Shotgun	56	41
LoombarR_2017	Adv. fibrosis	Shotgun	14	72
NagySzakalD_2017	ME/CFS	Shotgun	50	50
NielsenHB_2014	IBD	Shotgun	81	236
QinJ_2012	T2D	Shotgun	170	174
QinN_2014	Cirrhosis	Shotgun	123	114
RaymondF_2016	Cephalosporins	Shotgun	36	36
RubelMA_2020	STH	Shotgun	89	86
SankaranarayananK_2015	T2D	Shotgun	19	18
ThomasAM_2018a_CRC	CRC	Shotgun	29	24
ThomasAM_2018a_adenoma	Adenoma	Shotgun	27	24
ThomasAM_2018b	CRC	Shotgun	32	28
ThomasAM_2019_c	CRC	Shotgun	40	40
VogtmannE_2016	CRC	Shotgun	52	52
WirbelJ_2018	CRC	Shotgun	60	65
XieH_2016_asthma	Asthma	Shotgun	24	177
XieH_2016_migraine	Migraine	Shotgun	49	177
YachidasS_2019_CRC	CRC	Shotgun	258	251
YachidasS_2019_adenoma	Adenoma	Shotgun	67	251
YeZ_2018	BD	Shotgun	20	45
YuJ_2015	CRC	Shotgun	74	54
ZellerG_2014_CRC	CRC	Shotgun	53	61
ZellerG_2014_adenoma	Adenoma	Shotgun	42	61
ZhuF_2020	Schizophrenia	Shotgun	90	81

Abbreviations: ACVD = atherosclerotic cardiovascular disease; BD = Behcet's disease; CRC = colorectal cancer; IBD = inflammatory bowel disease; IGT = impaired glucose tolerance; ME/CFS = myalgic encephalomyelitis/chronic fatigue syndrome; PD = Parkinson's disease; STH = soil-transmitted helminth infection; T1D = type 1 diabetes; T2D = type 2 diabetes.

Construction of null datasets

To evaluate the error rate of the compared methods, we constructed a set of null datasets where no true (population level) prevalence differences exist between the groups.

For this, we utilized the healthy control groups from the original datasets. We restricted the selection to the studies including at least 20 healthy control samples. This resulted in 48 eligible “control datasets”.

From each of these 48 control datasets, we generated 10 independent null datasets by randomly partitioning the samples into artificial “case” and “control” groups. The sample sizes for these groups were determined using a two-step randomization process: for each iteration, there was a 50% probability that the samples were split evenly (balanced groups) and a 50% probability that the split size was randomized, subject to the constraint that both groups included at least 10 samples. Consistent with the main analyses, features present in fewer than four samples in a given null dataset were excluded.

FDR control in the null datasets

The false discovery rate (FDR) is defined as the expected proportion of false positive findings among all (statistically) significant findings:

$$\text{FDR} = E \left[\frac{V}{R} \right],$$

where V is the number of false positive findings and R is the total number of significant findings. By definition, if no significant findings are made ($R = 0$), the ratio is set to 0 ($\frac{V}{R} = 0$) [15].

In the null datasets, no true prevalence differences exist. Consequently, every significant finding is a false positive. Thus, if any significant findings are made ($R > 0$), it follows that $V = R$ and thus $\frac{V}{R} = 1$. Therefore:

$$\text{FDR} = P(R > 0) \cdot E \left[\frac{V}{R} \mid R > 0 \right] + P(R = 0) \cdot 0 = P(R > 0) \cdot 1 + 0 = P(R > 0).$$

Thus, in the null datasets, the FDR is equivalent to the probability of making at least one significant finding (i.e., the family-wise error rate). Consequently, if significance is based on a procedure that controls FDR at level α , the procedure is expected to yield significant findings in at most $\alpha \cdot 100\%$ of the null datasets.

Construction of the pairs of datasets in replication analysis

The dataset pairs in the replication analysis were constructed from the 80 original datasets by pairing those that investigated the same disease and utilized the same sequencing technology (16S or shotgun).

We excluded datasets with fewer than 10 samples in either the case or control group. Additionally, HIV datasets were excluded due to strong confounding effects reported in previous literature, and the non-CDI diarrhea dataset (*cdi_schubert_diarrhea*) was excluded because it utilized the same healthy control subjects as the other diarrhea dataset (*cdi_schubert_cdi*) from the same study.

The filtering resulted in 49 datasets (22 16S datasets and 27 shotgun datasets) for which at least one matching pair was available. From these datasets, a total of 110 dataset pairs were formed. The number of datasets and dataset pairs by sequencing type and disease are shown in Table 4. (Note that N datasets yield $\binom{N}{2} = \frac{N(N-1)}{2}$ dataset pairs.)

Table 4: Number of datasets and dataset pairs included in the replication analysis.

Disease	Datasets	Pairs
<i>16S sequencing</i>		
Adenoma	2	1
ASD	2	1
CRC	5	10
Diarrhea	3	3
IBD	4	6
Obesity (OB)	4	6
Overweight (OW)	2	1
(<i>Total</i>)	22	28
<i>Shotgun sequencing</i>		
Adenoma	5	10
CRC	11	55
IBD	5	10
T1D	2	1
T2D	4	6
(<i>Total</i>)	27	82
Total	49	110

Abbreviations: ASD = autism spectrum disorder; CRC = colorectal cancer; IBD = inflammatory bowel disease; OB = obesity; OW = overweight; T1D = type 1 diabetes; T2D = type 2 diabetes.

Proportion of significant findings in the original datasets

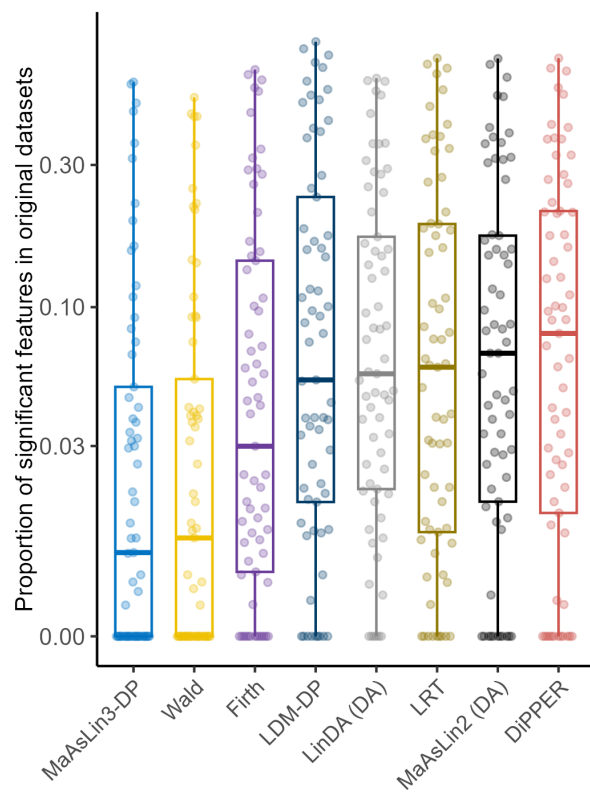


Figure 7: The proportion of significant findings in each of the 80 original datasets. Note the logarithmic scale. The methods are ordered by the median proportion of significant findings.

Performance of DiPPER with alternative hyperprior specifications and a Bayesian version of MaAsLin2

To assess the robustness of DiPPER to the choice of hyperpriors $\tau_0 \sim \text{HalfNormal}(0, 1^2)$ and $\nu_0 \sim \text{Laplace}(\mu_{\nu_0} = 0.50, \tau_{\nu_0} = 0.05)$, we evaluated its performance using four alternative hyperprior specifications:

- **DiPPER-Symm:** The skewness parameter is fixed to $\nu_0 = 0.50$, enforcing a symmetric Laplace prior for the differential prevalence estimates β_j .
- **DiPPER-Skewed:** The prior for the skewness parameter ν_0 is set to Beta(5, 5). Compared to the default Laplace(0.50, 0.05) prior, this distribution is less concentrated around $\nu_0 = 0.50$, allowing the skewness of the asymmetric Laplace prior for β_j to vary more freely.
- **DiPPER-Wide:** The prior for the scale parameter τ_0 is widened to HalfNormal(0, 2²), allowing the width of the asymmetric Laplace prior for β_j to vary more freely.
- **DiPPER-Narrow:** The prior for τ_0 is narrowed to HalfNormal(0, 0.5²), thereby constraining the width of the asymmetric Laplace prior more tightly.

In addition, we evaluated the performance of a Bayesian adaptation of the differential abundance analysis method MaAsLin2, denoted as **BMaAsLin2**. This method retained the identical hierarchical prior structure for the effect sizes β_j as the default version of DiPPER (Equations 2.1–2.6) but employed a Gaussian likelihood suitable for continuous data. The response variables y_{ij} were the standardized log-transformed relative abundances of taxonomic features:

$$y_{ij} \sim \mathcal{N}(\alpha_j + \beta_j \times \text{group}_i + \dots, \sigma_j^2).$$

The prior for the residual standard deviation was specified as $\sigma_j \sim \text{Gamma}(1, 1)$.

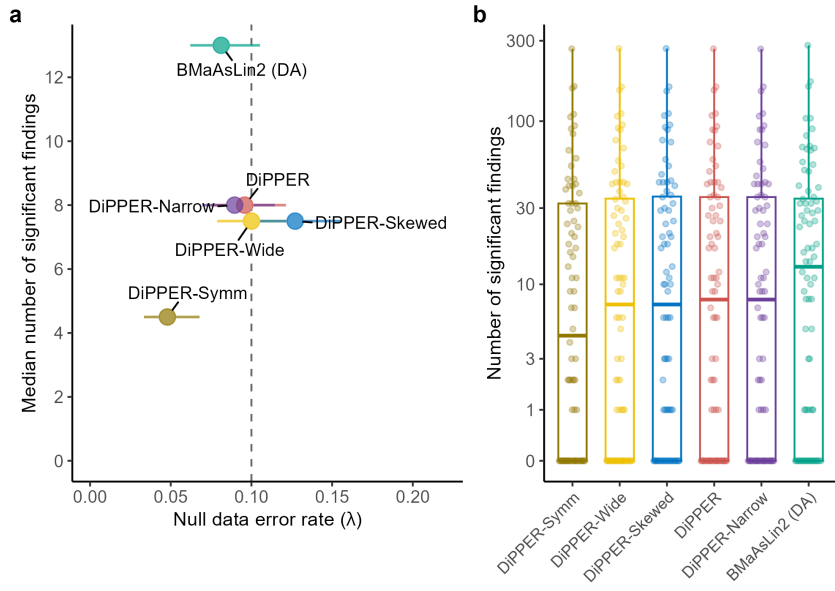


Figure 8: Performance of DiPPER with alternative hyperpriors and “Bayesian MaAsLin2” in the null and original datasets. **a)** Null data error rate (x-axis) versus sensitivity (median number of findings, y-axis). **b)** Distribution of the number of significant findings detected. This figure is analogous to Figure 4 in the main text.

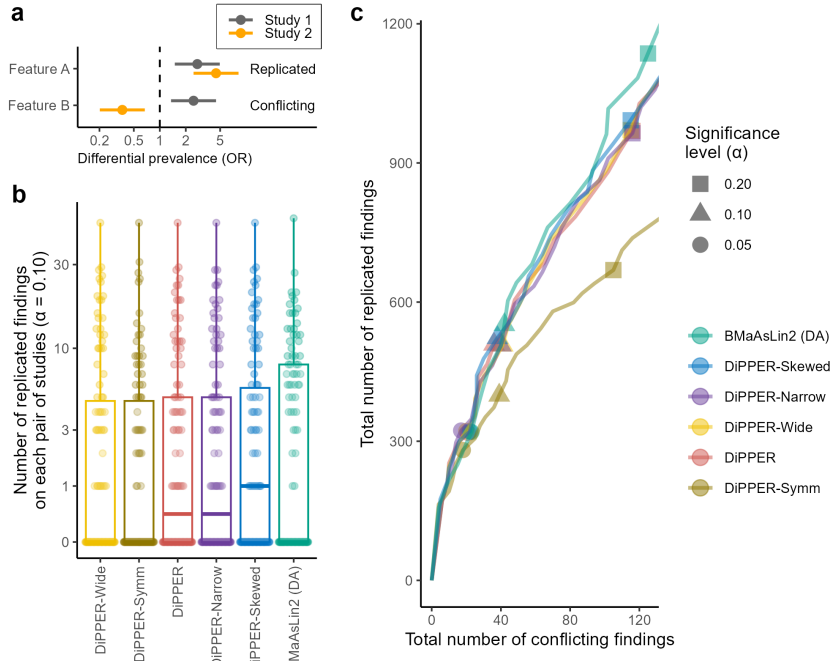


Figure 9: Performance of DiPPER with alternative hyperpriors and “Bayesian MaAsLin2” in the replication analysis. **a)** Illustration of replicated and conflicting results. **b)** Number of replicated results per study pair. **c)** Total replicated results versus conflicting results. This figure is analogous to Figure 5 in the main text.

Main results using significance level 0.05

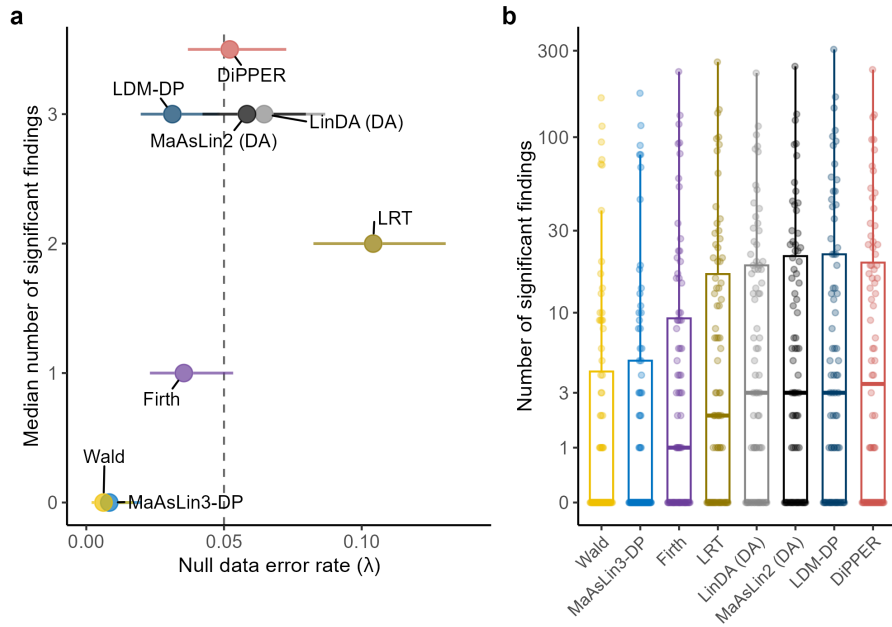


Figure 10: This figure is analogous to Figure 4 in the main text but significance level $\alpha = 0.05$ is used.

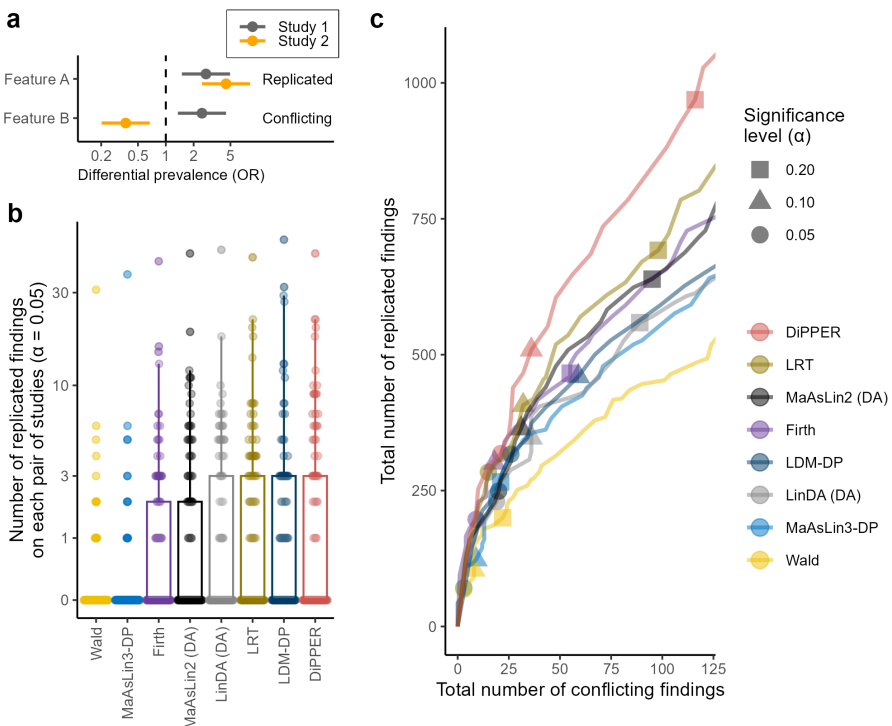


Figure 11: This figure is analogous to Figure 5 in the main text but significance level $\alpha = 0.05$ is used in b).